Msp1 cooperates with the proteasome for extraction of arrested mitochondrial import intermediates

Marion Basch[a], Mirjam Wagner[a], Stéphane Rolland[a], Andres Carbonell[a], Rachel Zeng[b], Siavash Khosravi[c], Andreas Schmidt[d], Wasim Aftab[d], Axel Imhof[d], Johannes Wagener[e], Barbara Conradt[a], and Nikola Wagener[a,b,*]

[a]Zell- und Entwicklungsbiologie, Department Biologie II, [c]Zellbiologie–Anatomie III, Biomedizinisches Centrum, and [d]Protein Analysis Unit ZfP, Ludwig-Maximilians-Universität München, Planegg-Martinsried 82152, Germany; [b]Max-Planck-Institut für Biochemie, Martinsried 82152, Germany; [e]Institut für Hygiene und Mikrobiologie, Julius-Maximilians-Universität Würzburg, Würzburg 97080, Germany

ABSTRACT **The mitochondrial AAA ATPase Msp1 is well known for extraction of mislocalized tail-anchored ER proteins from the mitochondrial outer membrane. Here, we analyzed the extraction of precursors blocking the import pore in the outer membrane. We demonstrate strong genetic interactions of Msp1 and the proteasome with components of the TOM complex, the main translocase in the outer membrane. Msp1 and the proteasome both contribute to the removal of arrested precursor proteins that specifically accumulate in these mutants. The proteasome activity is essential for the removal as proteasome inhibitors block extraction. Furthermore, the proteasomal subunit Rpn10 copurified with Msp1. The human Msp1 homologue has been implicated in neurodegenerative diseases, and we show that the lack of the *Caenorhabditis elegans* Msp1 homologue triggers an import stress response in the worm, which indicates a conserved role in metazoa. In summary, our results suggest a role of Msp1 as an adaptor for the proteasome that drives the extraction of arrested and mislocalized proteins at the mitochondrial outer membrane.**

Monitoring Editor
Benjamin Glick
University of Chicago

Received: Jun 17, 2019
Revised: Jan 31, 2020
Accepted: Feb 4, 2020

INTRODUCTION

One important step for mitochondrial biogenesis is the import of proteins into the organelle. The TOM complex is the essential translocase in the mitochondrial outer membrane and is involved in biogenesis of proteins destined for all mitochondrial subcompartments. After passage of the TOM complex, proteins take specific pathways sorting them to their final destination. The SAM complex inserts β-barrel proteins from the intermembrane space (IMS) side into the outer membrane; the TIM23 complex guides proteins with an N-terminal targeting signal into the matrix or the inner membrane; the TIM22 complex inserts highly hydrophobic proteins into the inner membrane; the MIA pathway traps soluble, cysteine-rich proteins in the IMS; and Oxa1 inserts inner membrane proteins from the matrix side (Neupert and Herrmann, 2007; Wiedemann and Pfanner, 2017).

Biogenesis of mitochondria and maintenance of mitochondrial homeostasis involve many complex processes that must be tightly regulated and coordinated. Recently, it was suggested that Msp1 (mitochondrial sorting of proteins) is involved in import quality control in mitochondria (Weidberg and Amon, 2018). Msp1 was first identified by Nakai *et al.* (1993) as an outer mitochondrial membrane (OMM) protein that belongs to the AAA (ATPases associated with various cellular activities) protein family. Msp1 is anchored

This article was published online ahead of print in MBoC in Press (http://www.molbiolcell.org/cgi/doi/10.1091/mbc.E19-06-0329) on February 12, 2020.

The authors declare that they have no conflict of interests.

Author contributions: N.W. conceived the study and wrote the manuscript; M.B., S.R., and N.W. designed the experiments; M.B., S.R., M.W., R.Z., S.K., A.C., A.S., and N.W. performed the experiments and analyzed the results; W.A. provided analysis software for mass spectrometric experiments; M.B., S.R., A.I., J.W., B.C., and N.W. discussed the data; J.W. and B.C. critically revised the manuscript; all authors read and approved the manuscript before submission.

*Address correspondence to: Nikola Wagener (wagener@bio.lmu.de).

Abbreviations used: AAA, ATPases associated with various cellular activities; GET, Guided Entry of TA proteins; GIP, general import pore; IMS, intermembrane space; Msp1, mitochondrial sorting of proteins; OMM, outer mitochondrial membrane; PMSF, phenylmethylsulfonyl fluoride; TA, tail-anchor; TOM, translocase in the mitochondrial outer membrane; UPR, unfolded protein response.

in the OMM by a single transmembrane domain and forms homohexameric complexes analogous to canonical AAA proteins (Wohlever *et al.*, 2017). It is highly conserved throughout evolution, which suggests an important role in cell homeostasis. Mutations in the mammalian homologue *ATAD1*/thorase are linked to neurological disorders (Zhang *et al.*, 2011; Piard *et al.*, 2018). In 2014, two independent studies demonstrated that Msp1 localizes to mitochondria and peroxisomes. At mitochondria, Msp1 eliminates mislocalized tail-anchored (TA) ER proteins from the outer membrane that accumulate when certain components of the Guided Entry of TA proteins pathway are missing (Chen *et al.*, 2014; Okreglak and Walter, 2014). At peroxisomes it fulfills a similar function. TA proteins that are not assembled into their target complexes become substrate of Msp1 and are removed from the peroxisomal membrane (Weir *et al.*, 2017). Very recently, a similar selection mechanism was proposed for TA proteins in the mitochondrial OMM (Dederer *et al.*, 2019). A study on mitochondrial compromised protein import response demonstrated the existence of a Pdr3-dependent mechanism that is activated when general protein import into mitochondria is disturbed by overexpression of TIM23 substrates destined for the inner membrane (Weidberg and Amon, 2018). In this study, Msp1 was identified as a factor that improves mitochondrial import under these stress conditions.

Here, we dissected the role of Msp1 and the proteasome in mitochondrial import quality control at the outer membrane. We demonstrate functional cooperation among the TOM complex, Msp1, and the proteasome in this context. By using an artificial TOM substrate, we uncover a cooperative mechanism of Msp1 and the proteasome in the extraction of TOM-clogging precursors and demonstrate the physical interaction of the proteasome, Msp1 and the precursor. Furthermore, we demonstrate that in the nematode *Caenorhabditis elegans* the Msp1 homologue MSPN-1 also functionally interacts with mitochondrial protein import, which suggests a similar conserved role of Msp1/MSPN-1 in metazoa.

RESULTS

MSP1 genetically interacts with several components of the TOM complex

The role of Msp1 in extraction of TA ER proteins from mitochondria and peroxisomes had been well described. We asked whether it might also have a function with respect to endogenous mitochondrial proteins. Since Msp1 is localized in the OMM and based on its supposed role in import quality control, we suspected a functional interaction with the TOM complex. The TOM complex is composed of seven different subunits of which Tom40 is essential for cell viability (Baker *et al.*, 1990) and Tom22 deletion results in a particularly sick mutant (Lithgow *et al.*, 1994; van Wilpe *et al.*, 1999). Tom40 forms the general import pore (GIP; Vestweber *et al.*, 1989; Hill *et al.*, 1998), which is in close contact with Tom22 and the three small Tom proteins Tom5, Tom6, and Tom7 (TOM core complex; Dekker *et al.*, 1998; Bausewein *et al.*, 2017; Araiso *et al.*, 2019; Tucker and Park, 2019). Deletion of one of the small Tom proteins results in a mild growth phenotype under normal conditions. On deletion of *TOM6*, the TOM complex partially falls apart while deletion of TOM7 rather stabilizes the complex (Hönlinger *et al.*, 1996; Dekker *et al.*, 1998). In contrast, deletion of *TOM5* has no effect on the overall amount of assembled complex, but still results in severe import deficiency (Kassenbrock *et al.*, 1993; Alconada *et al.*, 1995; Hönlinger *et al.*, 1996; Dietmeier *et al.*, 1997; Dekker *et al.*, 1998). The receptor proteins Tom20 and Tom70 are less tightly associated with the TOM core complex (Dekker *et al.*, 1998) and deletions of these subunits are normally well tolerated (Baker *et al.*, 1990; Lithgow *et al.*, 1994; Figure 1A). Tom22 also exhibits receptor properties in its charged N terminus exposed to the cytosol but, additionally, contributes significantly to the stability and functional organization of the whole complex (van Wilpe *et al.*, 1999; Model *et al.*, 2008, Shiota *et al.*, 2015).

We generated a set of *tom* deletion mutants and tested for decreased viability in the Δ*msp1* background. Specifically, we generated single and double mutants that lack only *MSP1* or *MSP1* and *TOM5*, *TOM6*, *TOM22*Δ3′UTR, *TOM20*, *TOM70*, or *TOM40*Δ3′UTR. Growth of these strains was analyzed at 30°C and 37°C by drop dilution assays (Figure 1A). We could observe a genetic interaction of *MSP1* with *TOM5, TOM20*, and *TOM40*Δ3′UTR, respectively, but not with *TOM6, TOM22*Δ3′UTR, or *TOM70* (Figure 1A).

On the basis of our observations, we speculated that the divergent genetic interactions are linked to the disruption of different steps of the import process mediated by the TOM complex (Ryan *et al.*, 2000). To further investigate this, we tested the accumulation of Hsp60 precursor, a well-characterized substrate of the TOM complex (Singh *et al.*, 1990), in the TOM mutants. As shown in Figure 1B, higher amounts of accumulated precursor coincide with a more severe growth defect. To exclude the possibility that additional deletion of *MSP1* affects the stability of the TOM complex in affected *tom* mutants further and therefore the protein import via TOM, we analyzed TOM stability at 30°C and 37°C in those mutants via Blue Native PAGE. At either temperature, deletion of *MSP1* did not result in instability of the TOM complex that could prevent efficient protein import (Figure 1C).

The restriction of precursor accumulation to certain TOM mutants indicates fundamental differences regarding the mechanism that removes precursors from the complex. We hypothesize that TOM mutants with impaired protein import, but weak or no precursor accumulation (i.e., Δ*tom6*, *TOM22*Δ3′UTR, Δ*tom70*, (Steger *et al.*, 1990; Alconada *et al.*, 1995; Nakai and Endo, 1995) (Figure 1B), show no genetic interaction because the precursor proteins never enter the import pore, get rapidly degraded in the cytosol, and thereby do not clog the import machinery. However, TOM mutants, which might partially import the precursor (Δ*tom5*, Δ*tom20, TOM40*Δ3′UTR; Figure 1B), depend on Msp1 being functional.

TOM dysfunction triggers *MSP1* expression

Survival of dysfunctional protein import at the level of TOM essentially depends on Msp1. Therefore, a regulatory response that induces Msp1 expression on TOM malfunction would be beneficial. We therefore checked whether deletion of *TOM5* affects Msp1 levels in vivo. Whole cell lysates were generated and probed for endogenous Msp1 levels. As shown in Figure 1D, Msp1 levels were increased in Δ*tom5* cells, indicating an up-regulation of Msp1 to compensate import deficiency. Next, we investigated whether lack of Msp1 itself affects biogenesis of other mitochondrial proteins, which could explain the effects we observed. To this end, we analyzed the endogenous levels of various mitochondrial proteins in whole cell lysates of the Δ*tom5*, Δ*msp1*, and Δ*tom5*Δ*msp1* mutants. Deletion of *TOM5* resulted in slightly reduced levels of Tim23 and Mia40 levels appeared slightly increased in the double mutant. Besides this, no other mitochondrial protein that we analyzed was affected in the mutant. Deletion of *MSP1* had no effect on endogenous protein levels, neither in the wild type nor in the Δ*tom5* background (Figure 1E). On the basis of these results, we conclude that the synthetic sickness of Δ*tom5*Δ*msp1* is not due to generally altered levels of other mitochondrial proteins in the Δ*msp1* background.

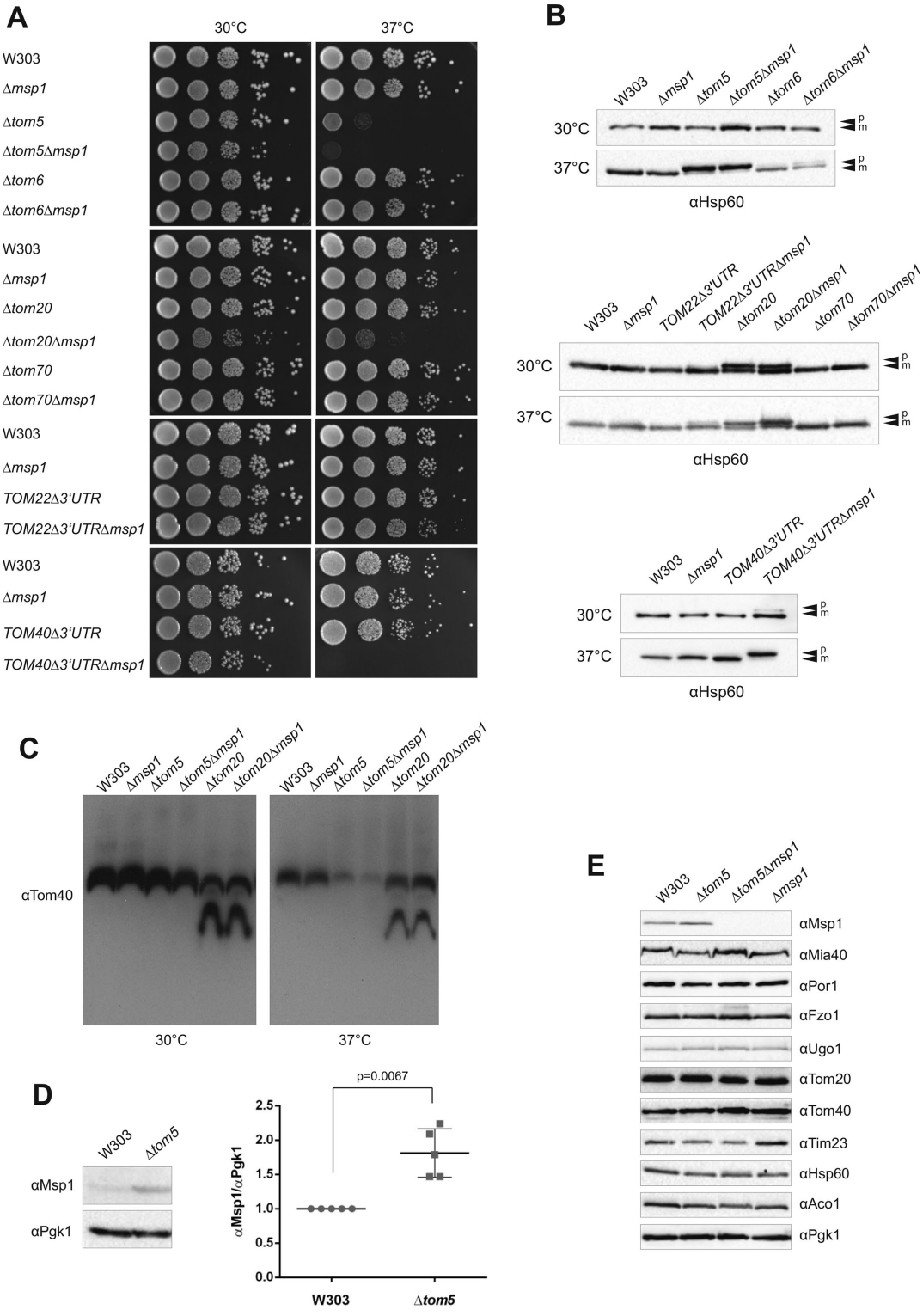

FIGURE 1: Genetic interaction analysis of *MSP1* and genes encoding the subunits of the TOM complex. (A) indicated strains were grown on YPD medium at 30°C and 37°C. All drops were spotted in a serial dilution of 1:10. (B) Analysis of the levels of precursor and mature form of the chaperonin Hsp60 at 37°C and 30°C in *tom* mutants by SDS–PAGE, Western blot and immunodecoration. (C) Stability of the TOM complex in the indicated mutants was analyzed by Blue Native PAGE and immunodecoration against Tom40. (D) Msp1 expression levels in wild type and the Δ*tom5* mutant. Protein levels of Msp1 and cytosolic Pgk1 were analyzed in wild type and the Δ*tom5* mutant, and quantification of the Msp1 expression levels relative to Pgk1 was performed. Error bars indicate standard deviations. The difference between the two strains is statistically significant by the one sample *t* test ($p = 0.0067$, $n = 5$). (E) The strains were grown on glucose-containing medium at 30°C. Whole cell extracts were analyzed for levels of the outer membrane proteins Msp1, Por1, Fzo1, Ugo1, Tom20, Tom40, the inner membrane proteins Tim23 and Mia40, and the matrix proteins Aco1 and Hsp60. Pgk1 was decorated as cytosolic control.

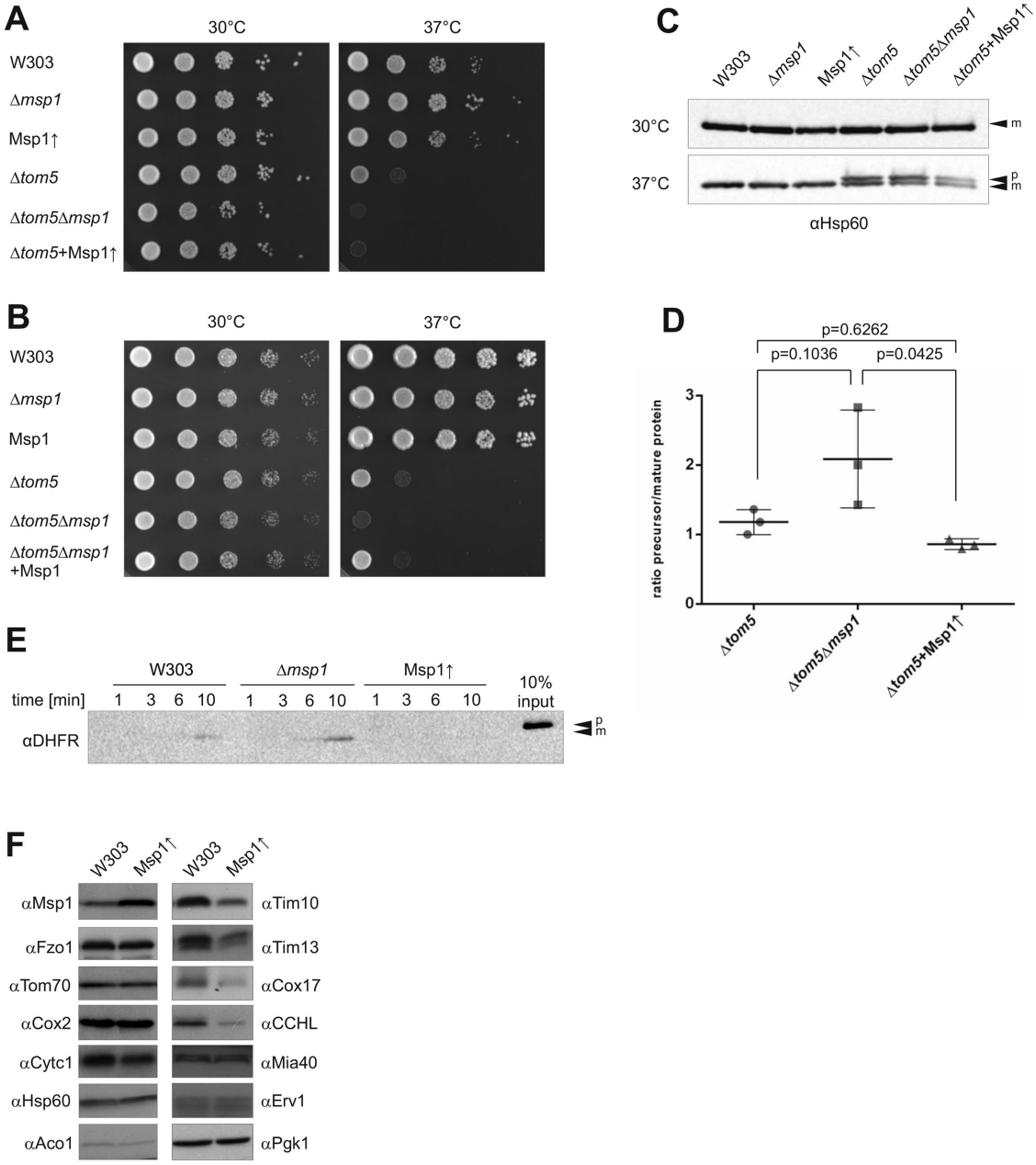

FIGURE 2: Analysis of *tom5* and *msp1 mutants*. (A, B) Complementation analysis with an Msp1 overexpression plasmid (A) and Msp1 expression from a plasmid under the endogenous promoter (B) on glucose-containing selective medium at 30° and 37°C. The dots were spotted in a serial dilution of 1:10. (C) Protein levels of the precursor (p) and mature (m) form of the chaperonin Hsp60 at 30° and 37°C in Δ*tom5* mutants with various Msp1 expression levels and (D) quantification of three independent experiments. Error bars indicate standard deviations. Statistical significance was tested by two-way ANOVA with the Tukey's multiple comparison test. (E) In organello import of unfolded Cytb2ΔTM-DHFR into isolated mitochondria. After indicated time points, mitochondria were washed and analyzed by SDS–PAGE, Western blot and immunodecoration. (F) Western blot analysis of endogenous protein levels showing proteins affected in Msp1 overexpressing cells.

Msp1 overexpression affects cell growth and mitochondrial protein import

Since Msp1 levels were increased approximately twofold in the Δ*tom5* mutant, we tested whether overexpression of Msp1 rescues the Δ*tom5* growth phenotype at 37°C. We therefore expressed Msp1 from a high-copy plasmid under a constitutive promoter and analyzed its effect on growth (Figure 2A). Unexpectedly, overexpression of Msp1 did not complement the Δ*tom5* growth phenotype; instead it diminished cell viability compared with the Δ*tom5* background. To make sure that our previous observations were due to the genetic interaction of *TOM5* and *MSP1*, we expressed Msp1 from a single-copy plasmid under its endogenous promoter (Figure 2B). As expected, growth of the Δ*tom5*Δ*msp1* mutant was restored in this strain to Δ*tom5* single mutant levels showing that deletion of *MSP1* causes the additional growth deficiency. The Msp1 expression level in the strains containing the high-copy

plasmid is approximately eightfold higher than the expression in the Δ*tom5* mutant (Supplemental Figure S1). This demonstrates that excessive abundance of Msp1 is harmful to cells.

To further investigate the interaction of Tom5 and Msp1, we analyzed the levels of precursor and mature form of endogenous Hsp60 in Δ*tom5*, Δ*tom5*Δ*msp1*, and Δ*tom5* Msp1 overexpressing cells at 30°C and 37°C (Figure 2, C and D). In these strains no precursor accumulated at 30°C. At 37°C, Hsp60 precursor was clearly visible and quantification revealed stronger accumulation of precursor in the Δ*tom5*Δ*msp1* cells. Interestingly, the total amount of Hsp60 seemed to be reduced in cells overexpressing Msp1 (Figure 2C). To address this issue, we isolated mitochondria of these three strains and performed an in organello import assay (Figure 2E). We used recombinantly expressed Cytb2-ΔTM-DHFR, an artificial substrate for mitochondrial matrix import that can be used to clog the TOM complex by previous irreversible folding of the DHFR domain (Koll *et al.*, 1992; Gold *et al.*, 2017). Following the import of the unfolded protein for 10 min revealed a severely decreased ability of mitochondria from Msp1 overexpressing cells to import the precursor. In contrast, cells lacking Msp1 showed increased import efficiency. To test whether this phenomenon might also be visible in the Msp1 overexpressing strain in vivo, we generated whole cell lysates and probed for various mitochondrial protein levels (Figure 2F). Interestingly, endogenous levels of probed IMS proteins were particularly affected while other mitochondrial proteins showed normal endogenous levels. Notably, several IMS proteins such Tim9 and Tim10 are essential, which could explain the harmful effect of Msp1 overexpression on cell growth.

Clearance of accumulated precursor proteins depends on Msp1

To further dissect the function that Msp1 exerts in cells that accumulate mitochondrial precursor proteins, we performed precursor chase experiments. Mitochondria were isolated from wild type, Δ*msp1*, and Msp1 overexpressing yeast strains. As substrate we used recombinantly expressed Cytb2-ΔTM-DHFR that was prefolded with methotrexate. The substrate was bound to isolated mitochondria and mitochondria were reisolated after 3 min. Samples were subsequently washed, either immediately or after 20 or 60 min, to remove unbound substrate and further analyzed for the amount of remaining Cytb2-ΔTM-DHFR precursor (Figure 3A). The amount of Cytb2-ΔTM-DHFR precursor after 20 min was considerably higher on mitochondria isolated from Δ*msp1* and after 3 min already strongly reduced on mitochondria isolated from the Msp1 overexpressing strain. This shows that precursor protein that is not able to pass the TOM complex is removed from mitochondria in an Msp1-dependent manner.

To test our hypothesis in vivo, we expressed Cytb2-ΔTM-DHFR under the *GAL1* promoter in Δ*tom5*, Δ*tom5*Δ*msp1* and Δ*tom5* cells overexpressing Msp1 in the presence of aminopterin to catalyze irreversible folding of the DHFR moiety in the cytosol (Figure 3B). The Δ*tom5* background was employed to enable prefolding of Cytb2-ΔTM-DHFR more efficiently. After 4 h, cells were shifted to glucose containing medium to stop Cytb2-ΔTM-DHFR expression and whole cell lysates were prepared after the indicated time points to monitor precursor accumulation. First, we observed a considerable amount of processed Cytb2-ΔTM-DHFR in all strains. However, the ratio of precursor to mature form was higher in the cells lacking Msp1. Second, regarding the chase of the precursor, we also observed its stabilization in the Δ*tom5*Δ*msp1* background. These results indicate that Msp1 removes proteins that clog the TOM translocase and thereby block efficient import of mitochondrial proteins in vivo.

MSPN-1 plays a role in mitochondrial quality control in *C. elegans*

The mammalian homologue *ATAD1*/thorase was shown to be required for regulation of synaptic activity in mice brain and thereby affecting learning and memory in *ATAD1* null mice (Zhang *et al.*, 2011). In humans, a homozygous *ATAD1* mutation in three patients resulted in severe encephalopathy and early death at the age of 3, 5, and 6 mo (Piard *et al.*, 2018). The study by Chen and colleagues (2014) demonstrated that a large fraction of *ATAD1*/thorase, as its yeast homologue, localizes to mitochondria. Depletion of *ATAD1* resulted in mitochondrial damage and accumulation of mislocated TA proteins on mitochondria. We therefore asked whether Msp1 homologues in metazoa fulfill a similar function as Msp1 in yeast.

C. elegans is a well-established model organism for the analysis of the unfolded protein response (UPR^{mt}). The transcription factor ATFS-1, which is under nonstress conditions normally imported and degraded in the mitochondria, transduces the signal from mitochondria to the nucleus on deficient protein import and is therefore a critical player in this pathway (Nargund *et al.*, 2012). It was recently proposed by Rolland and colleagues that compromised mitochondrial import acts as a signal to activate UPR^{mt} and evidence was presented that the mitochondrial targeting sequence of ATFS-1 functions as the sensor (Rolland *et al.*, 2019). We analyzed the induction of a $P_{hsp\text{-}6}$*GFP* reporter, which is induced by ATFS-1 during UPR^{mt} (Nargund *et al.*, 2012; Rolland *et al.*, 2019), in animals carrying the deletion *tm3831* in the gene *mspn-1* gene encoding a *C. elegans* homologue of Msp1. In the *mspn-1*(*tm3831*) mutant, the predicted MSPN-1 protein is lacking amino acids 47–136, which include the Walker A motif of the AAA domain. As shown in Figure 3, C and D, expression of the GFP reporter is three times higher in animals carrying the *mspn-1*(*tm3831*) mutation as compared with wild type. To exclude that the increased expression level is due to other mutations in the background, we generated an additional strain carrying the *mspn-1*(*tm3831*) mutation and the $P_{hsp\text{-}6}$*GFP* transcriptional reporter and confirmed the higher level of $P_{hsp\text{-}6}$*GFP* expression (Supplemental Figure S2). This demonstrates that the UPR^{mt} pathway is induced in *mspn-1* mutant animals. On the basis of our results and on the recent results of Rolland and colleagues (Rolland *et al.*, 2019), we propose that *C. elegans* MSPN-1 plays a similar role for the maintenance of mitochondrial import as in yeast.

Msp1 physically interacts with TOM-clogging substrate and the proteasome

Our data demonstrate the importance of Msp1 in clearing the clogged TOM complex. This raises the question whether Msp1 directly interacts with the translocase-trapped precursor. It was previously reported that a mutated variant of Msp1 that is unable to hydrolyze ATP (Msp1E193Q), but not the wild-type protein, is efficiently trapped with its substrates (Chen *et al.*, 2014; Okreglak and Walter, 2014). We therefore coexpressed His-tagged Cytb2-ΔTM-DHFR and the ATP hydrolysis mutant Msp1E193Q in the Δ*tom5*Δ*msp1* background (Figure 4A). Expression of Cytb2-ΔTM-DHFR-His was performed in the absence and presence of aminopterin either to allow complete import or to prefold Cytb2-ΔTM-DHFR-His in the cytosol to clog the TOM translocase. Subsequent NiNTA affinity purification of folded Cytb2-ΔTM-DHFR-His resulted in copurification of the TOM complex subunit Tom40, but not of Tom70. Besides this, notable amounts of Msp1E193Q could be copurified with prefolded Cytb2-ΔTM-DHFR-His, but only traces without prefolding of DHFR. Interaction of Msp1E193Q with unfolded Cytb2-ΔTM-DHFR-His could be explained by challenge of the TOM complex due to the substrate's massive overexpression.

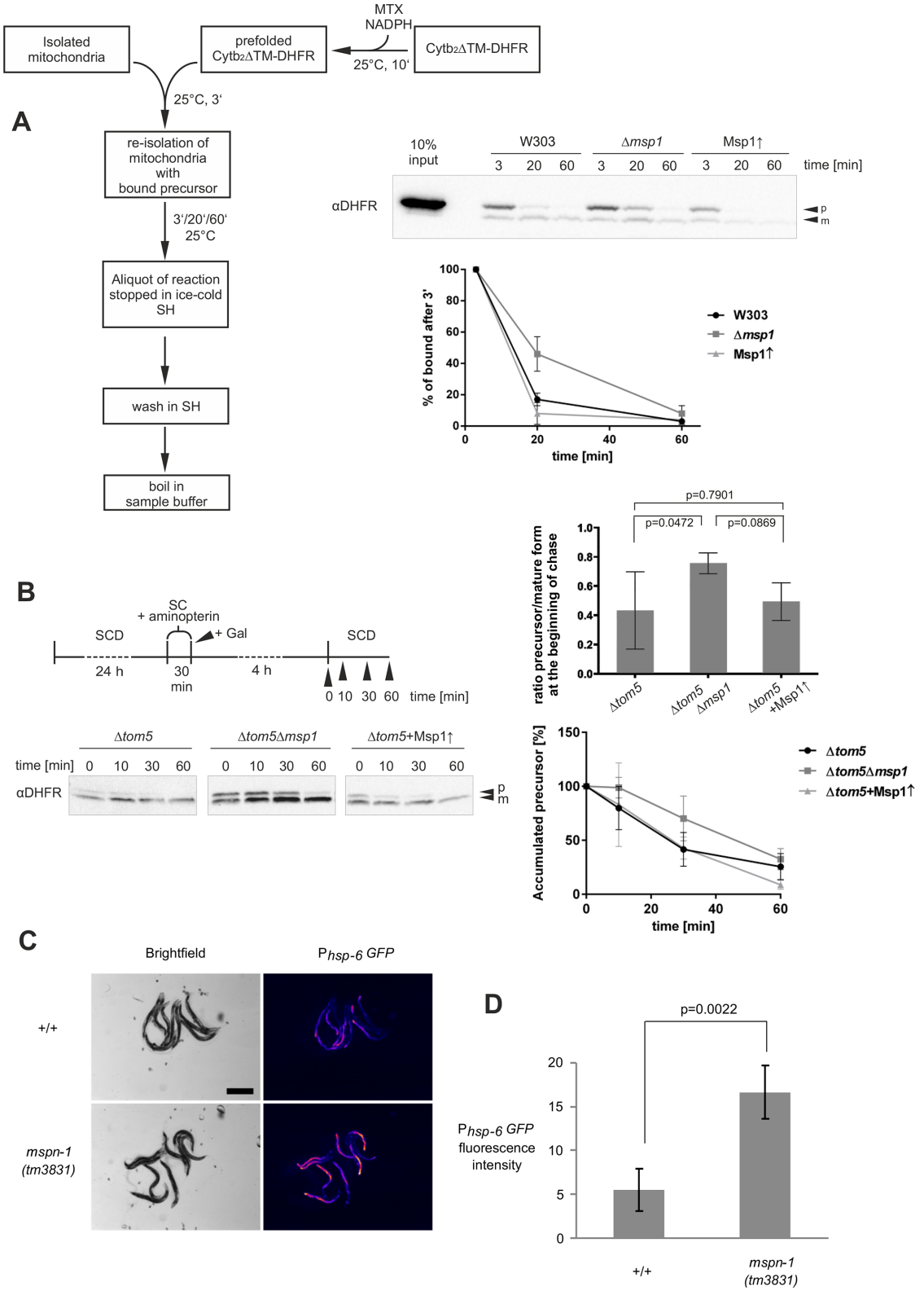

FIGURE 3: Msp1-dependent chase of folded precursor from the TOM complex and its functional conservation in *C. elegans*. (A) Recombinant Cytb2-ΔTM-DHFR was prefolded in the presence of methotrexate and bound to mitochondria of the indicated strains. After indicated time points mitochondria were reisolated, washed and analyzed by SDS–PAGE, Western blot and immunodecoration and quantified ($n = 3$). Unprocessed precursor was loaded as Total (T). Error bars indicate standard deviations. (B) Cytb2-ΔTM-DHFR was expressed under the *GAL1* promoter and prefolded in the presence of aminopterin in the indicated strains. After indicated time points, aliquots were taken from the cultures. Whole cell extracts were prepared and analyzed by SDS–PAGE, Western blot and immunodecoration. Cytb2-ΔTM-DHFR was quantified and chase and precursor/mature form ratio at the beginning of the chase were plotted ($n = 3$). Statistical

Lack of the TOM subunit in this elution fraction suggests a TOM-independent interaction.

Prompted by these observations, we asked whether we could find other interaction partners of Msp1 that are involved in this quality control mechanism. We therefore performed NiNTA affinity purification experiments with His-tagged Msp1 followed by mass spectrometric analyses. All proteins identified in these analyses are listed in Supplemental Table S1. The proteasomal subunit Rpn10 was copurified in three independent experiments (Figure 4B). Msp1 itself does not contain an annotated protease domain and we assumed that it cannot degrade its substrates on its own. Hence, these findings suggest that the proteasome is recruited to the mitochondrial surface in proximity to Msp1 to immediately degrade extracted proteins. Additional evidence for an Msp1-dependent recruitment of the proteasome to the mitochondrial surface was obtained from an experiment in which we analyzed gradient-purified mitochondria for the amount of bound proteasome. Considerably less proteasome copurified with mitochondria obtained from a Δ*msp1* mutant compared with the wild type (Supplemental Figure S3A).

TOM complex-clogging proteins are extracted in a proteasome-dependent manner

Since proteasomal substrates are typically marked by ubiquitin for selective degradation, we determined the overall amount of ubiquitinated proteins on mitochondria that were isolated from wild type, Δ*msp1*, and Msp1 overexpressing cells grown at 30°C. Under these conditions, *MSP1* is not crucial for cell viability (Figure 2A). In the mitochondria isolated from Msp1 overexpressing cells, the overall amount of ubiquitinated protein was reduced while there was only a slight difference between wild type and Δ*msp1* (Figure 4C). To check whether Msp1-specific substrates are ubiquitinated, we constructed yeast strains constitutively expressing chromosomally His-tagged or untagged ubiquitin and Cytb2-ΔTM-DHFR under the *GAL1* promoter. Cells of these strains were grown in the presence or absence of aminopterin in galactose containing medium, harvested, and lysed under denaturing conditions to perform NiNTA purification of ubiquitinated proteins. As shown in Figure 4D, we were able to purify a ubiquitinated form of Cytb2-ΔTM-DHFR after cells were grown in the presence of aminopterin. This shows that Cytb2-ΔTM-DHFR, which clogs the TOM translocase, is ubiquitinated prior to degradation.

To obtain evidence that these substrates are finally degraded by the proteasome, we performed in vitro chase experiments in the presence of proteasome inhibitor MG-132. To this end we incubated isolated wild-type mitochondria with recombinantly expressed Cytb2-ΔTM-DHFR that was prefolded in the presence of methotrexate. After 20, 60, or 120 min, aliquots were taken and separated into mitochondrial pellet and supernatant and further analyzed for the amount of Cytb2-ΔTM-DHFR precursor (Figure 5A). Surprisingly, in the mitochondrial fraction Cytb2-ΔTM-DHFR precursor levels were strikingly affected in the presence of MG-132 compared with the control. Although a minor degree of extraction could be monitored, its efficiency was strongly reduced when the proteasome was inhibited. This suggests that a concerted action of Msp1 and the proteasome is required for the high efficiency of this quality control system. In agreement with this finding, we found that the in organello chase reaction is also delayed in mitochondria isolated from cells that were deleted for *RPN10* (Supplemental Figure S3B).

A concerted action of Msp1 and proteasome is further supported by genetic interactions among Tom5, Msp1, and Rpn10 (Figure 5B). Rpn10 is one of the nonessential subunits of the proteasome and located in the linker region between regulatory and core particle (Glickman *et al.*, 1998). Depletion of Rpn10 alone caused no effect either at 30°C or at an elevated temperature (Figure 5B). Notably, while additional deletion of *MSP1* resulted only in a very mild growth phenotype, double deletion of *TOM5* and *RPN10* showed phenotype comparable to the Δ*tom5*Δ*msp1* double mutant, particularly at 37°C. Consistently, the Δ*rpn10*Δ*tom5* mutant shows accumulation of precursors similar to the Δ*msp1*Δ*tom5* mutant (Figure 5C). Reminiscent of the role of Cdc48 at the endoplasmic reticulum, all our findings strongly support a model where Msp1 and the proteasome cooperate and in which Msp1 acts as a mediator in proteasomal-dependent removal of arrested precursor proteins at the mitochondrial TOM complex.

DISCUSSION

In recent years, it became clear that the functionality of many essential cellular processes depends on highly specialized quality control mechanisms. Quality control of mitochondria can occur at different levels. While autophagy is the last resort to eliminate a dysfunctional organelle, many other immediate and more specialized rescue mechanisms were identified: activation of retrograde signaling pathways such as the UPR in the endoplasmic reticulum or mitochondrion, the integrated stress response, or the mitochondrial retrograde response induces the expression of a specific set of target genes (often encoding chaperones or proteases) to maintain or reestablish the balance and functionality of the organelle. But the first rescue efforts occur on the molecular level where single proteins or complexes monitor the functionality of a specific process and step in as soon as a problem is detected. In this study, we focused on the import deficiency at the mitochondrial outer membrane translocase (TOM complex).

The TOM complex consists of multiple subunits that have specialized functions. While deletion of the major subunit Tom40 is lethal, deletion of the receptor subunits Tom70 and Tom20 can be tolerated (Baker *et al.*, 1990; Lithgow *et al.*, 1994; Figure 1A). *TOM22* deletion results in a particularly severe growth phenotype (van Wilpe *et al.*, 1999). Deletion of the small Tom proteins Tom5, Tom6, or Tom7 shows almost no growth phenotype under normal conditions (Hönlinger *et al.*, 1996). In the present study, we deciphered the particular import steps, whose disturbance is sensitive to dysfunction of Msp1 and the proteasome. We show a negative genetic interaction between *MSP1* and *TOM5*, *TOM20* and *TOM40*, respectively, but also between *TOM5* and *RPN10*. On the basis of our observations and in principal agreement with the recent hypothesis of Weidberg and Amon (2018), we provide evidence for a functional interaction between the TOM complex and Msp1.

significance was tested by two-way ANOVA with the Tukey's multiple comparison test. Error bars indicate standard deviations. (C) Wild-type (+/+) and *mspn-1*(*tm3831*) animals carrying the $P_{hsp\text{-}6}$*GFP* transcriptional reporter (strains MD4432 and MD4430, respectively) were analyzed by brightfield and fluorescence microscopy (scale bar indicates 0.5 mm; intensity scale 1–1000). (D) The $P_{hsp\text{-}6}$*GFP* fluorescence intensities were quantified. Error bars indicate standard deviations. The difference between the two strains is statistically significant by Mann–Whitney test ($p = 0.0022$; $n = 6$).

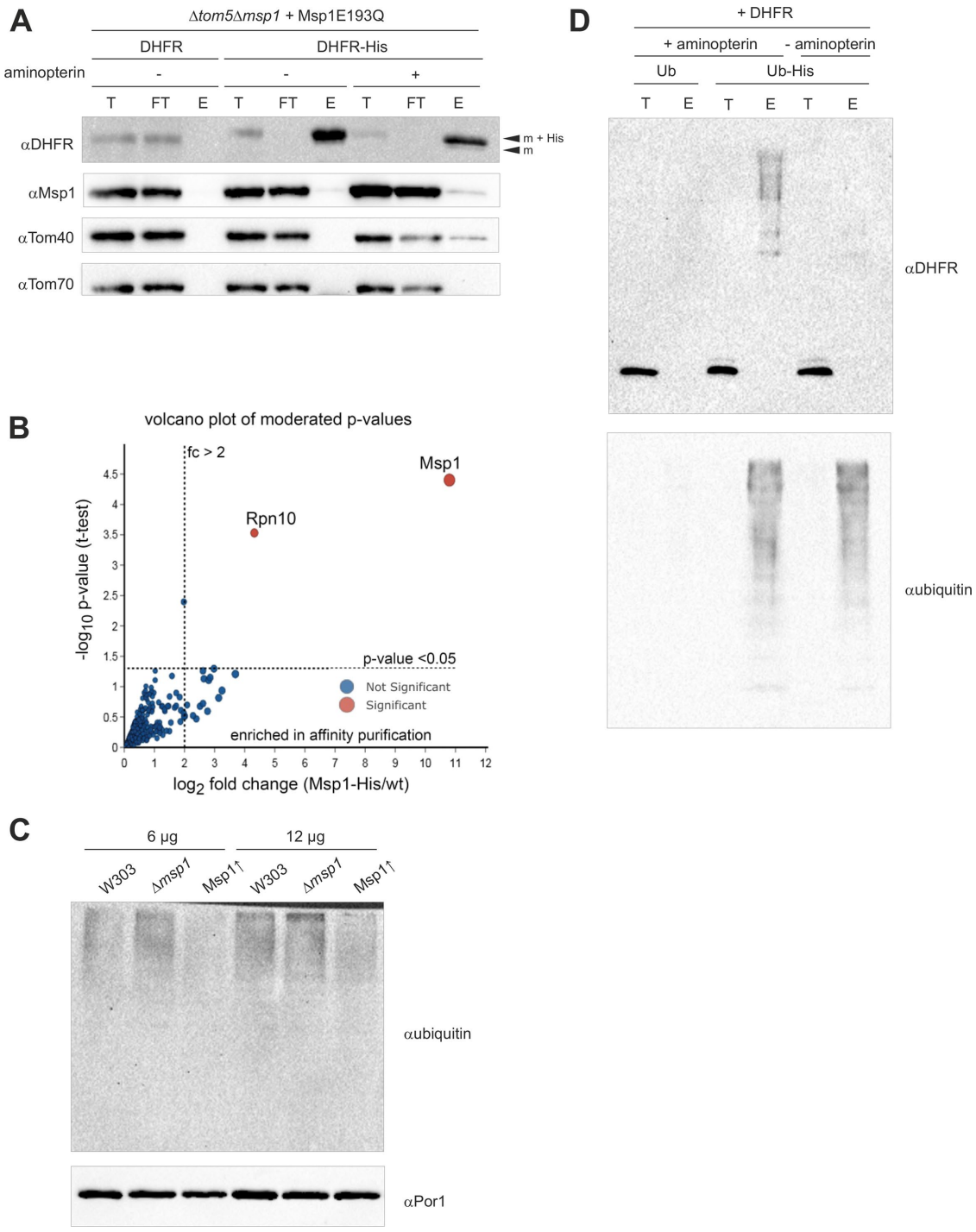

FIGURE 4: Identification of ubiquitin/proteasome system components in the quality control pathway at the TOM complex. (A) Cytb2-ΔTM-DHFR-His was expressed under the *GAL1* promoter and prefolded in the presence of aminopterin in the cultures. NiNTA affinity purification was performed with the isolated mitochondria and copurified proteins were identified by SDS–PAGE, Western blot and immunodecoration. (T, 10% total; FT, 10% flow through; E, 100% eluate) (B) Interacting proteins were analyzed by mass spectrometry-based proteomics after NiNTA purification and differences are depicted in the volcano plot after statistical comparison in Limma(R). The bait protein Msp1-His is most abundantly enriched with an enrichment factor (log2 fold change) of 11 in the top right corner. The strongest interactor is the proteasomal protein Rpn10, which was exclusively found in the Msp1-His interactome and not in the wild type control. (C) Isolated mitochondria were analyzed by SDS–PAGE, Western blot, and decorated against ubiquitin. (D) Strains expressing chromosomally integrated His-tagged ubiquitin and Cytb2-ΔTM-DHFR were grown in the presence and absence of aminopterin. Cells were collected and lysed. The cell lysate was subjected to NiNTA affinity purification and 0.5% total (T) and 100% bound fraction (Eluate [E]) were analyzed by SDS–PAGE, Western blot, and immunodecoration against DHFR and ubiquitin.

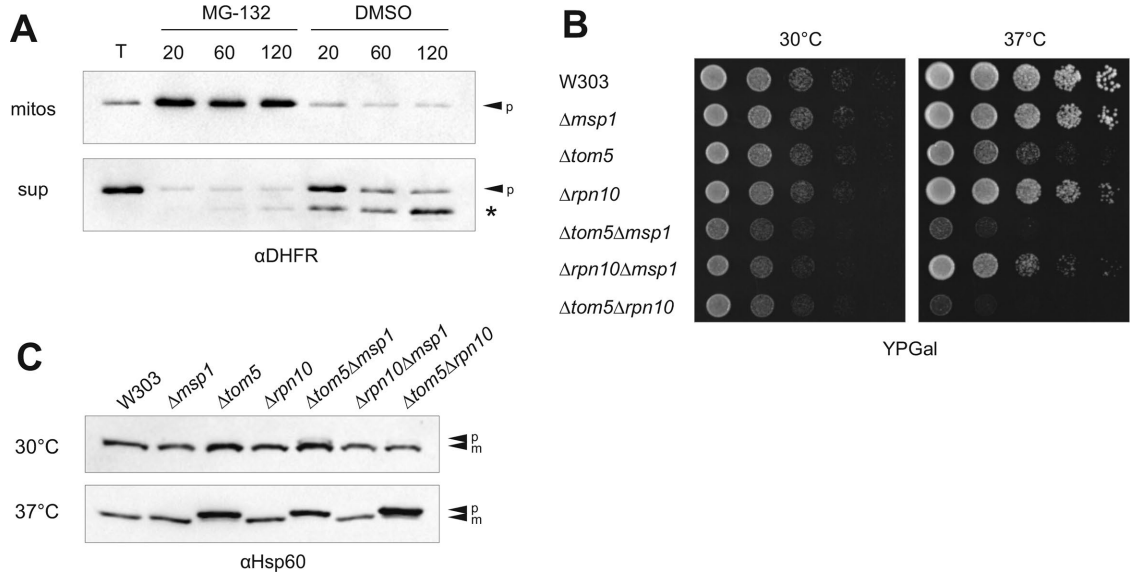

FIGURE 5: Proteasomal activity is required for extraction of arrested precursors. (A) Recombinant Cytb2-ΔTM-DHFR was prefolded in the presence of methotrexate and bound to wild-type mitochondria in the presence or absence of proteasome inhibitor MG-132. After indicated time points, mitochondria were reisolated and mitochondrial pellet and TCA-precipitated supernatant were analyzed by SDS–PAGE, Western blot, and immunodecoration against DHFR. (T, 10% of unprocessed Cytb2-ΔTM-DHFR precursor of each sample; a degradation product was labeled with an asterisk). (B) A growth analysis of the indicated yeast strains was performed on YPGal medium at 30°C or 37°C. Drops were spotted in serial dilution of 1:10. (C) Analysis of the levels of precursor and mature form of the chaperonin Hsp60 at 37° and 30°C by SDS–PAGE, Western blot, and immunodecoration.

Δ*tom5*Δ*msp1*, Δ*tom20*Δ*msp1*, and *TOM40*Δ3′UTRΔ*msp1* double mutants are synthetically sick as demonstrated by reduced growth rates at elevated temperatures. Importantly, we observed an accumulation of precursors in these mutants, but not in the Δ*tom6*Δ*msp1*, Δ*tom70*Δ*msp1*, and *TOM22*Δ3′UTRΔ*msp1* mutants that show no genetic interaction with *MSP1*. Our results allow for a deeper understanding of the different TOM complex subunits in cooperation with incoming precursors and their role for efficient import.

What distinguishes the two small TOM subunits Tom5 and Tom6 besides their genetic interaction with *MSP1*? Deletion of Tom5 has no effect on the overall amount of assembled TOM complex, but still results in severe import deficiency in vitro (Dietmeier *et al.*, 1997). It was demonstrated that incoming precursor proteins interact with Tom5 when they accumulate at the outer membrane (Dietmeier *et al.*, 1997). Further, Bausewein *et al.* (2017) showed the proximity of Tom5 to the cytosolic side of Tom40 and, in agreement with previously described findings, suggested Tom5 could serve as a docking platform for incoming precursors. Tom6 was located on the IMS side of the Tom40 (Bausewein *et al.*, 2017) and could not be cross-linked to the incoming precursors (Dietmeier *et al.*, 1997). In addition, for Tom7 it was demonstrated by two-step import that it is required at later steps during import at the *trans* site of the outer membrane and it is particularly important for proteins taking the SAM pathway to the outer membrane (Hönlinger *et al.*, 1996; Dietmeier *et al.*, 1997; Esaki *et al.*, 2004). In the Δ*tom5* mutant, which shows a strong genetic interaction with *MSP1*, precursors accumulate presumably at the pore of the TOM complex prior to translocation and thereby prevent further protein import. Consequently, and as shown in our study, these arrested precursors have to be removed by Msp1. The small subunits Tom6 and Tom7 are required for regulating the stability of the complex and, in case of Tom7, guiding the precursors after passage of the TOM complex. On deletion of *TOM6*, the TOM complex partially dissociates, which results in the release of the receptors from the core complex (Dekker *et al.*, 1998). The loss of receptor subunits will result in a TOM complex that most likely binds less import substrates; thus dysfunction will not be linked to accumulation at the import pore. This could explain why precursor accumulation and synthetic interaction is observed with the Δ*tom5* but not the Δ*tom6* mutant.

Why do we see specific accumulation of precursor in the Δ*tom20*, but not in the Δ*tom70* strain? Notably, both TOM subunits were reported to act as receptors for substrates in the protein import pathway. Furthermore, for both it was shown that Tom22 can partially compensate for their functions, although with strongly reduced efficiency (Harkness *et al.*, 1994). An explanation could be the different mechanisms that substrates of the individual receptors use to approach the TOM complex. Tom20 shows preferential binding affinity to mitochondrial N-terminal targeting signals, while Tom70 is a receptor for larger chaperone-guided precursors with internal targeting signals such as inner membrane carriers (Söllner *et al.*, 1989; Moczko *et al.*, 1993; Harkness *et al.*, 1994; Lithgow *et al.*, 1994). Binding of the Tom70 substrates to chaperones prior to the interaction with the TOM complex could prevent their arrest at the level of the outer membrane and result in their direct transfer to the precursor degradation system (Young *et al.*, 2003; Opalinski *et al.*, 2018). Consequently, Msp1 might not be required for their removal from the TOM translocase. Our results are very well in line with the recently reported organization of the TOM complex. Shiota *et al.* (2015) showed that Tom22 is required to modify the oligomeric state and thereby the import activity of the TOM complex. In cells depleted for Tom22, the TOM complex dissociates into the dimeric form. Importantly, the presence of Tom22 in the active complex is promoted by Tom6 (Sakaue *et al.*, 2019). Since Tom6 and Tom22 affect the composition and import competence of the TOM complex in a similar way, a comparable effect on precursor accumulation is expected.

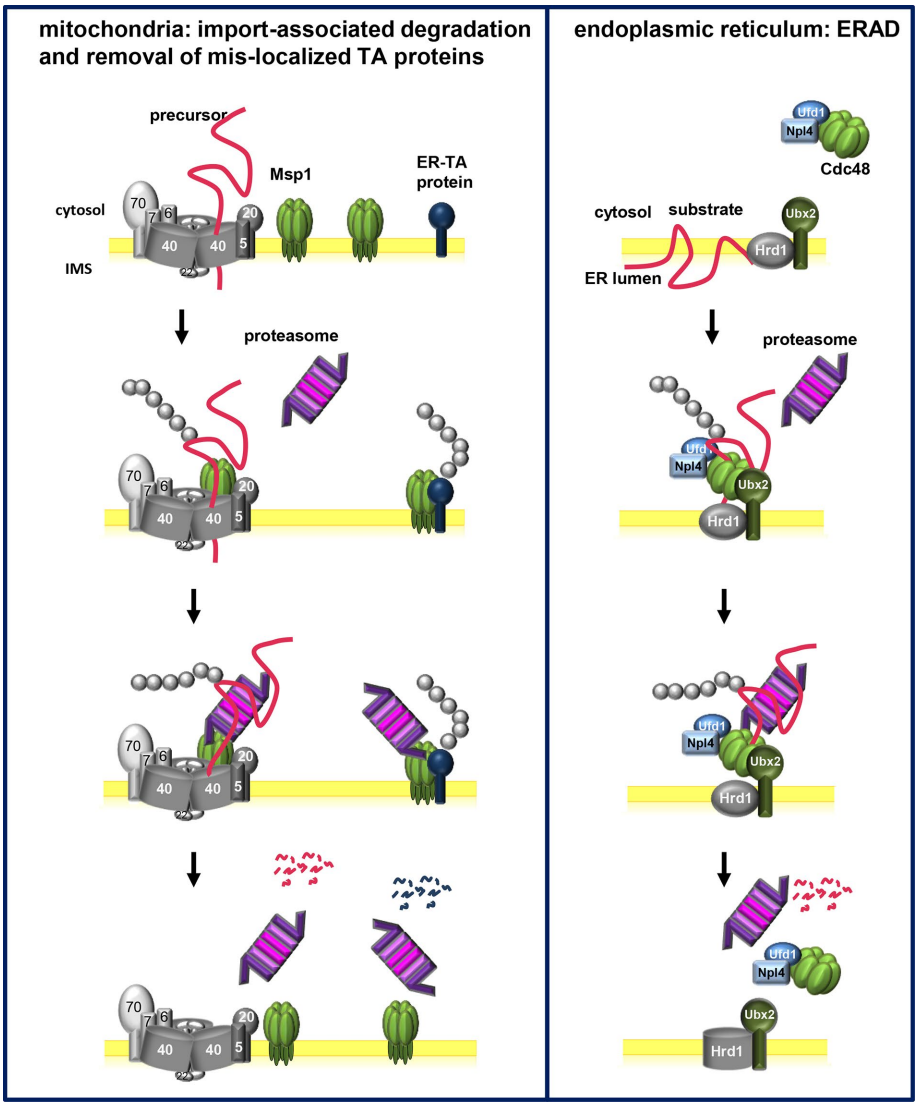

FIGURE 6: Model for the concerted action of Msp1 and the proteasome (similar to Cdc48 and proteasome function during ERAD) during extraction of Msp1 substrates. TOM subunits showing a genetic interaction with Msp1 are depicted in dark gray.

In addition to the genetic interactions between TOM subunits and *MSP1*, we observed a comparably strong interaction between *TOM5* and *RPN10*, which encodes a proteasomal subunit. Chase of arrested precursors from isolated mitochondria during inactivation of the proteasome revealed a strong dependency of the precursor extraction on proteasomal activity. Further, we showed the physical interaction between the proteasome and Msp1. On the basis of all our observations, we conclude a role of Msp1 and the proteasome in the same quality control mechanism at the mitochondrial import pore. We therefore propose that Msp1 recruits the proteasome and both then cooperate in the extraction of arrested precursors.

Interestingly, in the Msp1 overexpression mutant we found decreased levels of IMS proteins, which are substrates of the MIA pathway. Other proteins showed normal endogenous levels. Importantly, previous studies demonstrated that dysfunction of the MIA import pathway results in reduced levels of its substrate proteins (Chacinska *et al.*, 2004; Naoé *et al.*, 2004; Mesecke *et al.*, 2005; Terziyska *et al.*, 2005), while matrix protein precursors do not show affected endogenous protein levels on dysfunction of the TOM or TIM23 complex (Hönlinger *et al.*, 1996; Dietmeier *et al.*, 1997; Geissler *et al.*, 2002; Yamamoto *et al.*, 2002; Mokranjac *et al.*, 2003a,b; Waegemann *et al.*, 2015). This is probably due to the lower efficiency of IMS protein import. We therefore believe that overexpression of Msp1 shifts the equilibrium of IMS protein import toward the cytosolic pool, which is subsequently degraded. In agreement, a cellular response to accumulation of mitochondrial IMS proteins in the cytosol (UPRam) was described, which features degradation of accumulated IMS proteins in the cytosol by activating the proteasome (Wrobel *et al.*, 2015). Mildly increased levels of Mia40 in the Δ*tom5*Δ*msp1* mutant might also be a result of this response, and loss of essential IMS proteins in Msp1 overexpressing cells can explain the decreased viability because lack of IMS proteins is known for causing growth defects (Glerum *et al.*, 1996; Jarosch *et al.*, 1997; Paschen *et al.*, 2000). This observation is in agreement with the phenotype of the double mutant that overexpresses Msp1 in the Δ*tom5* background, which exhibits an unexpectedly strong growth defect (Figure 2A). Tom5 was reported to be of particular importance for import of small IMS proteins (Kurz *et al.*, 1999; Vögtle *et al.*, 2012; Gornicka *et al.*, 2014). In light of this specific function of Tom5, a genetic interaction between *TOM5* deletion and Msp1 overexpression seems plausible.

A recent study reported the response on massive cellular overload with Cytb2-ΔTM-DHFR, the same fusion protein we used in our study. Under these conditions that strongly resemble our experimental approach, a general up-regulation of proteasomal subunits was observed (Boos *et al.*, 2019), which is in agreement with our results.

Msp1 activity needs to be tightly regulated for being beneficial: overexpression impairs import, and reduced expression exacerbates TOM import deficiency. Interestingly and in line with these observations, a human neurological disorder was linked with a gain-of-function mutation in the gene encoding the human Msp1 homologue *ATAD1*/thorase (Piard *et al.*, 2018). Furthermore, a conserved role of Msp1 homologues of metazoans in mitochondrial protein import homeostasis is likely as loss of MSPN-1 function in *C. elegans* induces UPR^{mt}, a stress response that is induced on disturbed protein import (Rolland *et al.*, 2019).

On the basis of our results, we propose a model where both Msp1 and the proteasome act as key players during quality control of mitochondrial protein import at the TOM complex (Figure 6). Precursor proteins approach the OMM where those carrying an N-terminal signal sequence first get in contact with the receptor component Tom20. Then Tom5 would hand the protein over to the GIP Tom40. If the process is inhibited in one of these

steps, the import may come to a halt and result in clogging the TOM complex. Msp1 is required to catch the protein that clogs the import pore and disturbs mitochondrial biogenesis. We suggest that a similar mechanism applies to the Msp1-dependent removal of mislocalized TA ER proteins (Figure 6). The Msp1 substrate proteins subsequently undergo ubiquitination. Finally, the proteasome coordinately extracts the substrate together with Msp1 as inhibition of the proteasome activity significantly reduces extraction. In agreement with this model, Msp1 as well as proteasomal activity suppress the phenotypes that various TOM mutants exhibit due to the arrest of import. Our study defines a new and unexpected mechanism that relies on tight functional cooperation of Msp1 and the proteasome in mitochondrial quality control processes, which strongly resemble the ERAD pathway that is required for removal of misfolded proteins at the endoplasmic reticulum (Mayer *et al*., 1998; Walter *et al*., 2001; Ravid *et al*., 2006; Nakatsukasa *et al*., 2013).

Just recently, two independent studies reported the requirement of Doa10 in degradation of mislocalized TA ER proteins. In those cases, the Msp1 substrate was shown to relocate to the ER after extraction by Msp1 where it was ubiquitinated in a Ubc6-, Ubc7-, and Doa10-dependent manner (Dederer *et al*., 2019; Matsumoto *et al*., 2019). Interestingly, Msp1 seems to extract non-ubiquitinated substrate while Cdc48 seems to extract the substrate in its ubiquitinated form from the ER membrane (Matsumoto *et al*., 2019). Hints for differences between extraction of mislocalized TA proteins and extraction of other Msp1 substrates came from a study by Li *et al*. (2019) that addressed the role of specific residues in Msp1 and its substrates for extraction and degradation. They found that modification of a specific hydrophobic stretch in the model substrate Pex15Δ30 turns its degradation not only depending on Msp1 but also on the proteasome (Li *et al*., 2019). This observation supports our finding where arrested precursor proteins are removed in a proteasome-dependent manner. The recent discovery of Ubx2-dependent import quality control at the TOM channel (Mårtensson *et al*., 2019) can explain why the Msp1-dependent mechanism of arrested precursor removal is not essential for the cell to survive and not exclusive as observed in our in organello chase experiments. Particularly under unstressed conditions, Δ*msp1* mutants do not exhibit a growth phenotype. However, in line with our results, Mårtensson *et al*. observed the genetic interaction between *MSP1* and *UBX2* (Mårtensson *et al*., 2019), indicating that both encoded proteins act in two parallel pathways that ensure mitochondrial protein import quality control.

MATERIALS AND METHODS

Yeast strains

All mutants were generated in the *Saccharomyces cerevisiae* background W303α (MATα, *ade2-1, his3-11,15 leu2,112 trp1 ura23-53 can1-100*). In the Δ*msp1* mutant, the *MSP1* ORF was replaced by an *hph*MX cassette. *TOM5*, *TOM6*, *TOM20*, and *TOM70* ORFs were replaced by a *kan*MX4 cassette. The 3′UTRs of the essential genes *TOM22 and TOM40* were replaced by a *kan*MX4 cassette resulting in reduced expression of the respective genes. The strain expressing chromosomally tagged *MSP1* was generated by integration of a C-terminal His_7 tag in combination with a *kan*MX4 cassette for selection. For the generation of strains expressing His-tagged ubiquitin, the YIplac128-HisUbi plasmid (Kalocsay *et al*., 2009) was linearized with *EcoR*V and the DNA fragment was genomically integrated on transformation into yeast cells according to Gietz *et al*. (1995). All new strains were confirmed by PCR or immunoblotting.

Plasmids

For overexpression, the *MSP1* ORF was cloned into pYX242 (Novagen) by use of the *Nco*I and *Hin*dIII restriction sites. For endogenous expression levels, the *MSP1* ORF was cloned into pRS315 including 300 base pairs of the 5′ and 3′ UTR by use of the restriction sites *Not*I and *Xho*I. To introduce the E193Q point mutation into the ATPase domain of Msp1, both plasmids were amplified by use of Phusion Polymerase (NEB) and two primers carrying the desired mutation (5′-CAAGTTACAACCTTGTATAATATTCATTGACCAAATTGATTCATTCCTTAGAGAAC-3′ and 5′-GTTCTCTAAGGAATGAATCAATTTGGTCAATGAATATTATACAAGGTTGTAACTTG-3′). After *Dpn*I treatment, the PCR product was transformed directly into competent *Escherichia coli* DH5α cells for amplification.

All plasmids were sequenced by the Genomics Service Unit of the Faculty of Biology, LMU Munich.

The plasmids pYES2-Cytb_2(1-107)ΔTM-DHFR, pYES2-Cytb_2(1-167)ΔTM-DHFR, and pYES2-Cytb_2(1-167)ΔTM-DHFR-His_6 were received as a kind gift from Dejana Mokranjac (LMU Munich, Planegg-Martinsried, Germany) and described previously in Popov-Celeketic *et al.* (2008, 2011).

Preparation of whole cell extracts

For analysis of protein levels, whole cell extracts were prepared from liquid cultures by alkaline extraction as described in Kushnirov (2000). The final pellet was boiled in 50 µl 3× Laemmli buffer (150 mM Tris-HCl, 3 mM EDTA, 0.02% bromophenol blue, 30% glycerol, 6% SDS, and freshly added 6% β-mercaptoethanol, pH 6.8) for 5 min at 95°C.

Immunoblotting

Proteins were separated by 8, 12, or 16% SDS–PAGE and transferred onto Nitrocellulose membranes. After incubation with primary antibody overnight and secondary antibody (goat-anti-rabbit immunoglobulin G [IgG] horseradish peroxidase [HRP] [1:10,000] or goat anti-mouse IgG HRP [1:5000; Bio-Rad]) for 1 h at room temperature, signals were visualized in a Bio-Rad Gel Doc XR+Gel Documentation System.

Media

The *S. cerevisiae* strains were grown in YP, S, or SC drop-out medium. As carbon sources, 2% glucose, 2% galactose, 3% glycerol, or 2% lactate were added, if not indicated otherwise.

Isolation of mitochondria

Yeast cells were harvested in logarithmic growth phase by centrifugation. After washing with water, the cells were treated with 100 mM Tris (no pH adjusted) and 10 mM dithiothreitol (DTT) under shaking for 10 min at 30°C. Cell membranes were digested by zymolyase T20 (Amsbio) in 1.2 M sorbitol and 20 mM KH_2PO_4 (pH 7.4) for 1 h at 30°C. The cell pellet was washed twice in homogenization buffer (0.6 M sorbitol, 10 mM Tris, 1 mM EDTA, 0.2% fatty acid-free bovine serum albumin, and 1 mM phenylmethylsulfonyl fluoride [PMSF], pH 7.4). Spheroblasts were gently broken by pipetting with a cut 5-ml pipette tip in homogenization buffer. Mitochondria were collected from the supernatant of the lysed cells by centrifugation for 10 min at 12,000 rpm. The mitochondrial pellet was resuspended in SM buffer (0.6 M sorbitol, 20 mM MOPS-KOH, pH 7.2), aliquoted, and shock frozen in liquid N_2.

Expression and chase of mitochondrially targeted precursor protein in vivo

Yeast strains carrying pYES2-Cytb_2(1-107)ΔTM-DHFR constructs were kept in logarithmic growth phase in SLac medium containing 0.1% glucose to repress the *GAL1* promoter. The expression of Cytb_2(1-107)ΔTM-DHFR was induced in the same medium containing 1% galactose instead of glucose for 4 h at 37°C. The DHFR moiety of the protein was folded in the presence of 0.2 mM aminopterin (Sigma) during the entire expression time. After DHFR accumulation, the cells were again shifted to glucose instead of galactose to repress the expression and samples were taken at several time points to analyze the chase of the accumulated Cytb_2(1-107)ΔTM-DHFR. The samples at each time point were shock frozen, and whole cell extracts were prepared and analyzed by SDS–PAGE, Western blot, and immunodecoration against DHFR. The quantification was done with Image Lab Software from Bio-Rad.

Binding and chase of mitochondrially targeted precursor protein in vitro

Recombinant Cytb_2(1-167)ΔTM-DHFR was a kind gift from Dejana Mokranjac (Koll *et al.*, 1992; Gold *et al.*, 2017). It was prefolded in the presence of methotrexate and bound to isolated mitochondria of the respective strains. After indicated time points, either mitochondria were reisolated by centrifugation or the supernatant containing the unbound DHFR was trichloroacetic acid (TCA) precipitated. Both were washed and analyzed by SDS–PAGE, Western blot, and immunodecoration against DHFR. MG-132 was used at 100 µM final concentration in chase experiments where indicated.

Purification of Cytb_2ΔTM-DHFR-His after aminopterin treatment

Yeast cells carrying the pYES2-Cytb_2(1-167)ΔTM-DHFR-His_6 construct grown overnight in SLac medium containing 0.1% glucose. The next day cells were washed with water, resuspended in SLac medium, and pretreated with 0.2 mM aminopterin (Sigma) for 30 min. Afterward, 1% galactose was added to induce Cytb_2ΔTM-DHFR-His_6 expression. After 3 h incubation, the mitochondria were isolated according to the previously described protocol.

For purification of Cytb_2ΔTM-DHFR-His_6, 500 µg isolated mitochondria were pelleted and resuspended in Tris/MTX buffer (20 mM Tris, 80 mM KCl, 20 mM imidazol, 10% glycerol, 1 mM methotrexate, 8 mM NADPH, 1 mM PMSF, pH 7.4) and solubilized with 1% digitonin. After a clarifying spin, the supernatant was transferred to Ni-NTA Agarose beads (QIAGEN) and incubated for 1 h. Cytb_2ΔTM-DHFR was eluted with 3× Laemmli buffer containing 300 mM imidazol for 3 min at 95°C. The samples were analyzed by SDS–PAGE, Western blot, and immunodecoration.

Purification of ubiquitinated Cytb_2ΔTM-DHFR

The purification of ubiquitinated DHFR was performed under denaturing conditions. Cells (200 ODs) were harvested, washed with ice-cold water, and lysed with 1.91 N NaOH and 5% (vol/vol) β-mercaptoethanol. After 15 min incubation on ice, 55% TCA was added and incubated on ice for a further 15 min. The cells were pelleted, washed with ice-cold water, and afterward resuspended in buffer A (6 M guanidinium chloride, 100 mM NaH_2PO_4 H_2O, 10 mM Tris, pH 8.0) containing 0.05% Tween-20. To break the cells completely, the resuspended pellet was shaken vigorously for 3 h. For clarification, the suspension was centrifuged for 20 min at 23,000 × *g* at 4°C. The supernatant was supplemented with imidazole to a final concentration of 10 mM and transferred to 100 µl Ni-NTA Agarose beads (QIAGEN) for binding overnight at 4°C on a rotating wheel. The next day, the beads were washed three times with buffer A containing 0.05% Tween-20 and 10 mM imidazol. Afterward the beads were washed five times with buffer C (8 M urea, 100 mM NaH_2PO_4 H_2O, 10 mM Tris, pH 6.3) containing 0.05% Tween-20. The elution of bound proteins was performed with 30 µl 1% SDS at 65°C for 10 min, and the eluate was dried in a SpeedVac (Christ) at 45°C for 25 min. To the dried beads, 10 µl H_2O and 15 µl HU buffer (8 M Urea, 5% SDS, 200 mM Tris pH 6.8, Bromophenolblue, 1.5% DTT) were added and incubated at 65°C for 10 min. The input control was prepared from 1 OD of cells of the final culture, which were ruptured and lysed by vortexing with 10 µl H_2O, 15 µl HU buffer, and glass beads. The proteins were denatured at 65°C for 10 min.

Purification of His-tagged Msp1 for mass spectrometry analysis

Yeast cells bearing chromosomally His-tagged Msp1 were grown in synthetic medium containing 2% galactose. Cells were harvested and resuspended in 50 mM sodium phosphate, pH 8.0, 100 mM NaCl, 20 mM imidazol, 1:100 Protease Arrest Reagent (Calbiochem), and opened by vortexing with glass beads. Membranes were solubilized with 0.5% TritonX100 (Serva) and cell lysate was incubated with NiNTA Agarose beads (QIAGEN) for 1 h. For mass spectrometry analysis, the detergent was removed by washing three times with 50 mM NH_4HCO_3 (Serva).

LC-MS/MS short gradient analysis

For the identification of Msp1 interacting proteins, beads were resuspended in 4 M urea in 100 mM Tris, pH 7.5, to unfold proteins bound to the Ni-NTA resin. LysC (0.2 µg) for protein cleavage and 15 mM DTT for reduction of disulfide bonds was added to the suspension and the mixture was incubated at 27°C for 2 h. After 1 h of incubation, 35 mM iodoacetamide was added to block free sulfhydryl groups. After completion of the precleavage step, the sample mixture was diluted with 200 µl of 100 mM Tris, pH 7.5, and 1 µg of trypsin was added to cleave proteins to small oligopeptides for liquid chromatography/tandem mass spectrometry (LC-MS/MS) analysis. The obtained peptide mixture was separated from the beads and acidified with 10% TFA to a final concentration of 0.5% and a pH ~2.5. Stage tips were prepared with three disks of Empore C18 filter material (3M) as described earlier, and acidified peptides were desalted and subsequently vacuum dried. The samples were redissolved in 0.1% formic acid and directly loaded onto a 15-cm column with an inner diameter of 75 µm packed with 2.4-µm beads (Dr. Maisch GmbH, Reprosil C18-Aq) via the autosampler of the Thermo U3000 nano chromatography system (Thermo-Fisher Scientific). Peptides were separated and eluted using a linear gradient of 50 min from 3% ACN to 40% ACN in water/0.1% formic acid and directly sprayed into a benchtop Orbtitrap mass spectrometer (Q Exactive HF, Thermo Scientific). The mass spectrometer was operated in a data-dependent mode with survey scans acquired at 60,000 resolution (at m/z = 200) with an AGC target of 3E6. Based on the survey scan, up to 10 peptide features were selected and fragmented using HCD-based fragmentation at a normalized collision energy of 27 and fragmentation scans were acquired at a resolution of 15,000 (at m/z = 200). Previously fragmented peptides were dynamically excluded for 20 s within an m/z window of 10 ppm. Raw data were processed using the MaxQuant 1.5.5.1 computational platform (Cox and Mann, 2008). Peak lists generated were searched against the yeast Uniprot database with initial precursor and fragment mass

tolerance of 20 and 4 ppm for the first search and the main search steps, respectively. Carbamidomethylation of cysteine residues was enabled as fixed modification with oxidation of methionine and protein N-terminal acetylation as variable modification. Proteins were quantified using the LFQ intensity values, which were log2 transformed and median normalized. Contaminants, reversed hits, and protein hits with fewer than three values were excluded from the subsequent statistical analysis using the Limma algorithm within R (Ritchie *et al.*, 2015).

Statistical analysis of protein levels

Normal distribution was analyzed with the Kolmogorov–Smirnov test. If the data showed normal distribution, they were analyzed using the one sample *t* test. Statistical significance was tested by two-way analysis of variance (ANOVA) with Tukey's multiple comparison test.

Worm strains

The strain SJ4100, which carries the $P_{hsp\text{-}6}$*GFP* transcriptional reporter (Yoneda *et al.*, 2004), was used to monitor UPR^{mt} induction. The strain carrying the *mspn-1* deletion *tm3831* was generated by the National BioResource Project. The strain was backcrossed in total three times (one time with N2 and two times with SJ4100). At the end of the last backcross, two homozygous wild-type strains carrying for the $P_{hsp\text{-}6}$*GFP* reporter were isolated (MD4432 and MD4433). In addition, two *mspn-1*(*tm3831*) homozygous strains carrying the $P_{hsp\text{-}6}$*GFP* reporter were isolated (MD4430 and MD4431). These strains are isogenic with the exception of the presence of the *mspn-1*(*tm3831*) mutation.

Analysis of UPR^{mt} induction

Four L4 larvae of MD4432 and MD4433 (+/+; $P_{hsp\text{-}6}$*GFP*) as well as MD4430 and MD4431 (*mspn-1*(*tm3831*); $P_{hsp\text{-}6}$*GFP*) were inoculated on a NGM plate and incubated at 20°C. After 24 h, the four adults were transferred onto a new NGM plate and let to lay eggs for 4 h at 20°C. The adults were then removed from the plates and the plates were further incubated for 4 d at 20°C. F1 adults were analyzed by brightfield and fluorescence microscopy using a Leica GFP dissecting microscope (M205 FA) and the software Leica Application Suite (3.2.0.9652). Images were quantified using a Fiji macro as previously described (Rolland *et al.*, 2019). The experiment was performed blind.

Statistical analysis of UPR^{mt} induction

Equal variance was tested using the F-test, whereas normality was tested using the Shapiro–Wilk test. If the data showed equal variance but nonnormal distribution, we used a nonparametric Mann–Whitney test. If the data showed normal distribution but unequal variance, we used an unpaired *t* test with Welch's correction.

ACKNOWLEDGMENTS

We are very grateful to Sandra Esser, Fabian Köhler, and Mariam Museridze for technical assistance and help with experiments. We thank Shohei Mitani (National BioResource Project, Tokyo, Japan) for *mspn-1(tm3831)* and the *Caenorhabditis* Genetics Center (supported by the National Institutes of Health National Center for Research Resources) for strains. We are grateful to Dejana Mokranjac for providing purified Cytb2-ΔTM-DHFR and to Walter Neupert and Kai Hell for steady scientific advice. This work was financially supported by DFG grant WA3802/1-1, the LMUexcellent program of the Bundesexzellenztinitiative, the Förderprogramm für Forschung und Lehre of the Medical Faculty of the LMU Munich, and the Center for Integrated Protein Science Munich.

REFERENCES

Alconada A, Kubrich M, Moczko M, Honlinger A, Pfanner N (1995). The mitochondrial receptor complex: the small subunit Mom8b/Isp6 supports association of receptors with the general insertion pore and transfer of preproteins. Mol Cell Biol 15, 6196–6205.

Araiso Y, Tsutsumi A, Qiu J, Imai K, Shiota T, Song J, Lindau C, Wenz LS, Sakaue H, Yunoki K, *et al.* (2019). Structure of the mitochondrial import gate reveals distinct preprotein paths. Nature 575, 395–401.

Baker KP, Schaniel A, Vestweber D, Schatz G (1990). A yeast mitochondrial outer membrane protein essential for protein import and cell viability. Nature 348, 605–609.

Bausewein T, Mills DJ, Langer JD, Nitschke B, Nussberger S, Kühlbrandt W (2017). Cryo-EM structure of the TOM core complex from Neurospora crassa. Cell 170, 693–700.e7.

Boos F, Kramer L, Groh C, Jung F, Haberkant P, Stein F, Wollweber F, Gackstatter A, Zoller E, van der Laan M, *et al.* (2019). Mitochondrial protein-induced stress triggers a global adaptive transcriptional programme. Nat Cell Biol 21, 442–451.

Chacinska A, Pfannschmidt S, Wiedemann N, Kozjak V, Sanjuan Szklarz LK, Schulze-Specking A, Truscott KN, Guiard B, Meisinger C, Pfanner N (2004). Essential role of Mia40 in import and assembly of mitochondrial intermembrane space proteins. EMBO J 23, 3735–3746.

Chen YC, Umanah GK, Dephoure N, Andrabi SA, Gygi SP, Dawson TM, Dawson VL, Rutter J (2014). Msp1/ATAD1 maintains mitochondrial function by facilitating the degradation of mislocalized tail-anchored proteins. EMBO J 33, 1548–1564.

Cox J, Mann M (2008). MaxQuant enables high peptide identification rates, individualized p.p.b.-range mass accuracies and proteome-wide protein quantification. Nat Biotechnol 26, 1367–1372.

Dederer V, Khmelinskii A, Huhn AG, Okreglak V, Knop M, Lemberg MK (2019). Cooperation of mitochondrial and ER factors in quality control of tail-anchored proteins. Elife 8, e45506.

Dekker PJ, Ryan MT, Brix J, Muller H, Honlinger A, Pfanner N (1998). Preprotein translocase of the outer mitochondrial membrane: molecular dissection and assembly of the general import pore complex. Mol Cell Biol 18, 6515–6524.

Dietmeier K, Honlinger A, Bomer U, Dekker PJ, Eckerskorn C, Lottspeich F, Kubrich M, Pfanner N (1997). Tom5 functionally links mitochondrial preprotein receptors to the general import pore. Nature 388, 195–200.

Esaki M, Shimizu H, Ono T, Yamamoto H, Kanamori T, Nishikawa S, Endo T (2004). Mitochondrial protein import. Requirement of presequence elements and tom components for precursor binding to the TOM complex. J Biol Chem 279, 45701–45707.

Geissler A, Chacinska A, Truscott KN, Wiedemann N, Brandner K, Sickmann A, Meyer HE, Meisinger C, Pfanner N, Rehling P (2002). The mitochondrial presequence translocase: an essential role of Tim50 in directing preproteins to the import channel. Cell 111, 507–518.

Gietz RD, Schiestl RH, Willems AR, Woods RA (1995). Studies on the transformation of intact yeast cells by the LiAc/SS-DNA/PEG procedure. Yeast 11, 355–360.

Glerum DM, Shtanko A, Tzagoloff A (1996). Characterization of COX17, a yeast gene involved in copper metabolism and assembly of cytochrome oxidase. J Biol Chem 271, 14504–14509.

Glickman MH, Rubin DM, Fried VA, Finley D (1998). The regulatory particle of the Saccharomyces cerevisiae proteasome. Mol Cell Biol 18, 3149–3162.

Gold VA, Brandt T, Cavellini L, Cohen MM, Ieva R, van der Laan M (2017). Analysis of mitochondrial membrane protein complexes by electron cryo-tomography. Methods Mol Biol 1567, 315–336.

Gornicka A, Bragoszewski P, Chroscicki P, Wenz LS, Schulz C, Rehling P, Chacinska A (2014). A discrete pathway for the transfer of intermembrane space proteins across the outer membrane of mitochondria. Mol Biol Cell 25, 3999–4009.

Harkness TA, Nargang FE, van der Klei I, Neupert W, Lill R (1994). A crucial role of the mitochondrial protein import receptor MOM19 for the biogenesis of mitochondria. J Cell Biol 124, 637–648.

Hill K, Model K, Ryan MT, Dietmeier K, Martin F, Wagner R, Pfanner N (1998). Tom40 forms the hydrophilic channel of the mitochondrial import pore for preproteins [see comment]. Nature 395, 516–521.

Honlinger A, Bomer U, Alconada A, Eckerskorn C, Lottspeich F, Dietmeier K, Pfanner N (1996). Tom7 modulates the dynamics of the mitochondrial outer membrane translocase and plays a pathway-related role in protein import. EMBO J 15, 2125–2137.

Jarosch E, Rodel G, Schweyen RJ (1997). A soluble 12-kDa protein of the mitochondrial intermembrane space, Mrs11p, is essential for

mitochondrial biogenesis and viability of yeast cells. Mol Gen Genet 255, 157–165.
Kalocsay M, Hiller NJ, Jentsch S (2009). Chromosome-wide Rad51 spreading and SUMO-H2A.Z-dependent chromosome fixation in response to a persistent DNA double-strand break. Mol Cell 33, 335–343.
Kassenbrock CK, Cao W, Douglas MG (1993). Genetic and biochemical characterization of ISP6, a small mitochondrial outer membrane protein associated with the protein translocation complex. EMBO J 12, 3023–3034.
Koll H, Guiard B, Rassow J, Ostermann J, Horwich AL, Neupert W, Hartl FU (1992). Antifolding activity of hsp60 couples protein import into the mitochondrial matrix with export to the intermembrane space. Cell 68, 1163–1175.
Kurz M, Martin H, Rassow J, Pfanner N, Ryan MT (1999). Biogenesis of Tim proteins of the mitochondrial carrier import pathway: differential targeting mechanisms and crossing over with the main import pathway. Mol Biol Cell 10, 2461–2474.
Kushnirov VV (2000). Rapid and reliable protein extraction from yeast. Yeast 16, 857–860.
Li L, Zheng J, Wu X, Jiang H (2019). Mitochondrial AAA-ATPase Msp1 detects mislocalized tail-anchored proteins through a dual-recognition mechanism. EMBO Rep 20, e46989.
Lithgow T, Junne T, Suda K, Gratzer S, Schatz G (1994). The mitochondrial outer membrane protein Mas22p is essential for protein import and viability of yeast. Proc Natl Acad Sci USA 91, 11973–11977.
Mårtensson CU, Priesnitz C, Song J, Ellenrieder L, Doan KN, Boos F, Floerchinger A, Zufall N, Oeljeklaus S, Warscheid B, Becker T (2019). Mitochondrial protein translocation-associated degradation. Nature 569, 679–683.
Matsumoto S, Nakatsukasa K, Kakuta C, Tamura Y, Esaki M, Endo T (2019). Msp1 clears mistargeted proteins by facilitating their transfer from mitochondria to the ER. Mol Cell 76, 191–205.e10.
Mayer TU, Braun T, Jentsch S (1998). Role of the proteasome in membrane extraction of a short-lived ER-transmembrane protein. EMBO J 17, 3251–3257.
Mesecke N, Terziyska N, Kozany C, Baumann F, Neupert W, Hell K, Herrmann JM (2005). A disulfide relay system in the intermembrane space of mitochondria that mediates protein import. Cell 121, 1059–1069.
Moczko M, Gartner F, Pfanner N (1993). The protein import receptor MOM19 of yeast mitochondria. FEBS Lett 326, 251–254.
Model K, Meisinger C, Kuhlbrandt W (2008). Cryo-electron microscopy structure of a yeast mitochondrial preprotein translocase. J Mol Biol 383, 1049–1057.
Mokranjac D, Paschen SA, Kozany C, Prokisch H, Hoppins SC, Nargang FE, Neupert W, Hell K (2003a). Tim50, a novel component of the TIM23 preprotein translocase of mitochondria. EMBO J 22, 816–825.
Mokranjac D, Sichting M, Neupert W, Hell K (2003b). Tim14, a novel key component of the import motor of the TIM23 protein translocase of mitochondria. EMBO J 22, 4945–4956.
Nakai M, Endo T (1995). Identification of yeast MAS17 encoding the functional counterpart of the mitochondrial receptor complex protein MOM22 of Neurospora crassa. FEBS Lett 357, 202–206.
Nakai M, Endo T, Hase T, Matsubara H (1993). Intramitochondrial protein sorting. Isolation and characterization of the yeast MSP1 gene which belongs to a novel family of putative ATPases. J Biol Chem 268, 24262–24269.
Nakatsukasa K, Brodsky JL, Kamura T (2013). A stalled retrotranslocation complex reveals physical linkage between substrate recognition and proteasomal degradation during ER-associated degradation. Mol Biol Cell 24, 1765–1775.
Naoe M, Ohwa Y, Ishikawa D, Ohshima C, Nishikawa S, Yamamoto H, Endo T (2004). Identification of Tim40 that mediates protein sorting to the mitochondrial intermembrane space. J Biol Chem 279, 47815–47821.
Nargund AM, Pellegrino MW, Fiorese CJ, Baker BM, Haynes CM (2012). Mitochondrial import efficiency of ATFS-1 regulates mitochondrial UPR activation. Science 337, 587–590.
Neupert W, Herrmann JM (2007). Translocation of proteins into mitochondria. Annu Rev Biochem 76, 723–749.
Okreglak V, Walter P (2014). The conserved AAA-ATPase Msp1 confers organelle specificity to tail-anchored proteins. Proc Natl Acad Sci USA 111, 8019–8024.
Opaliński Ł, Song J, Priesnitz C, Wenz LS, Oeljeklaus S, Warscheid B, Pfanner N, Becker T (2018). Recruitment of cytosolic J-proteins by TOM receptors promotes mitochondrial protein biogenesis. Cell Rep 25, 2036–2043.
Paschen SA, Rothbauer U, Kaldi K, Bauer MF, Neupert W, Brunner M (2000). The role of the TIM8–13 complex in the import of Tim23 into mitochondria. EMBO J 19, 6392–6400.
Piard J, Umanah GKE, Harms FL, Abalde-Atristain L, Amram D, Chang M, Chen R, Alawi M, Salpietro V, Rees MI, *et al*. (2018). A homozygous ATAD1 mutation impairs postsynaptic AMPA receptor trafficking and causes a lethal encephalopathy. Brain 141, 651–661.
Popov-Celeketic D, Mapa K, Neupert W, Mokranjac D (2008). Active remodelling of the TIM23 complex during translocation of preproteins into mitochondria. EMBO J 27, 1469–1480.
Popov-Celeketic D, Waegemann K, Mapa K, Neupert W, Mokranjac D (2011). Role of the import motor in insertion of transmembrane segments by the mitochondrial TIM23 complex. EMBO Rep 12, 542–548.
Ravid T, Kreft SG, Hochstrasser M (2006). Membrane and soluble substrates of the Doa10 ubiquitin ligase are degraded by distinct pathways. EMBO J 25, 533–543.
Ritchie ME, Phipson B, Wu D, Hu Y, Law CW, Shi W, Smyth GK (2015). limma powers differential expression analyses for RNA-sequencing and microarray studies. Nucleic Acids Res 43, e47.
Rolland SG, Schneid S, Schwarz M, Rackles E, Fischer C, Haeussler S, Regmi S, Yeroslaviz A, Habermann B, Mokranjac D, *et al*. (2019). Compromised mitochondrial protein import acts as a signal for UPR^{mt}. Cell Rep 28, 1659–1669.e5.
Ryan MT, Wagner R, Pfanner N (2000). The transport machinery for the import of preproteins across the outer mitochondrial membrane. Int J Biochem Cell Biol 32, 13–21.
Sakaue H, Shiota T, Ishizaka N, Kawano S, Tamura Y, Tan KS, Imai K, Motono C, Hirokawa T, Taki K, *et al*. (2019). Porin associates with Tom22 to regulate the mitochondrial protein gate assembly. Mol Cell 73, 1044–1055.
Shiota T, Imai K, Qiu J, Hewitt VL, Tan K, Shen HH, Sakiyama N, Fukasawa Y, Hayat S, Kamiya M, *et al*. (2015). Molecular architecture of the active mitochondrial protein gate. Science 349, 1544–1548.
Singh B, Patel HV, Ridley RG, Freeman KB, Gupta RS (1990). Mitochondrial import of the human chaperonin (HSP60) protein. Biochem Biophys Res Commun 169, 391–396.
Sollner T, Griffiths G, Pfaller R., Pfanner N, Neupert W (1989). MOM19, an import receptor for mitochondrial precursor proteins. Cell 59, 1061–1070.
Steger HF, Sollner T, Kiebler M, Dietmeier KA, Pfaller R, Trulzsch KS, Tropschug M, Neupert W, Pfanner N (1990). Import of ADP/ATP carrier into mitochondria: two receptors act in parallel. J Cell Biol 111, 2353–2363.
Terziyska N, Lutz T, Kozany C, Mokranjac D, Mesecke N, Neupert W, Herrmann JM, Hell K (2005). Mia40, a novel factor for protein import into the intermembrane space of mitochondria is able to bind metal ions. FEBS Lett 579, 179–184.
Tucker K, Park E (2019). Cryo-EM structure of the mitochondrial protein-import channel TOM complex at near-atomic resolution. Nat Struct Mol Biol 26, 1158–1166.
van Wilpe S, Ryan MT, Hill K, Maarse AC, Meisinger C, Brix J, Dekker PJ, Moczko M, Wagner R, Meijer M, *et al*. (1999). Tom22 is a multifunctional organizer of the mitochondrial preprotein translocase. Nature 401, 485–489.
Vestweber D, Brunner J, Baker A, Schatz G (1989). A 42K outer-membrane protein is a component of the yeast mitochondrial protein import site. Nature 341, 205–209.
Vögtle FN, Burkhart JM, Rao S, Gerbeth C, Hinrichs J, Martinou JC, Chacinska A, Sickmann A, Zahedi RP, Meisinger C (2012). Intermembrane space proteome of yeast mitochondria. Mol Cell Proteomics 11, 1840–52.
Waegemann K, Popov-Celeketic D, Neupert W, Azem A, Mokranjac D (2015). Cooperation of TOM and TIM23 complexes during translocation of proteins into mitochondria. J Mol Biol 427, 1075–1084.
Walter J, Urban J, Volkwein C, Sommer T (2001). Sec61p-independent degradation of the tail-anchored ER membrane protein Ubc6p. EMBO J 20, 3124–3131.
Weidberg H, Amon A (2018). MitoCPR-A surveillance pathway that protects mitochondria in response to protein import stress. Science 360, aan41461.
Weir NR, Kamber RA, Martenson JS, Denic V (2017). The AAA protein Msp1 mediates clearance of excess tail-anchored proteins from the peroxisomal membrane. Elife 6, e28507.
Wiedemann N, Pfanner N (2017). Mitochondrial machineries for protein import and assembly. Annu Rev Biochem 86, 685–714.

Wohlever ML, Mateja A, McGilvray PT, Day KJ, Keenan RJ (2017). Msp1 is a membrane protein dislocase for tail-anchored proteins. Mol Cell 67, 194–202.e196.
Wrobel L, Topf U, Bragoszewski P, Wiese S, Sztolsztener ME, Oeljeklaus S, Varabyova A, Lirski M, Chroscicki P, Mroczek S, *et al*. (2015). Mistargeted mitochondrial proteins activate a proteostatic response in the cytosol. Nature 524, 485–488.
Yamamoto H, Esaki M, Kanamori T, Tamura Y, Nishikawa S, Endo T (2002). Tim50 is a subunit of the TIM23 complex that links protein translocation across the outer and inner mitochondrial membranes. Cell 111, 519–528.
Yoneda T, Benedetti C, Urano F, Clark SG, Harding HP, Ron D (2004). Compartment-specific perturbation of protein handling activates genes encoding mitochondrial chaperones. J Cell Sci 117(Pt 18), 4055–4066.
Young JC, Hoogenraad NJ, Hartl FU (2003). Molecular chaperones Hsp90 and Hsp70 deliver preproteins to the mitochondrial import receptor Tom70. Cell 112, 41–50.
Zhang J, Wang Y, Chi Z, Keuss MJ, Pai YM, Kang HC, Shin JH, Bugayenko A, Wang H, Xiong Y, *et al*. (2011). The AAA+ ATPase Thorase regulates AMPA receptor-dependent synaptic plasticity and behavior. Cell 145, 284–299.